e-J. Surf. Sci. Nanotech. Vol. 13 (2015) 435-439 Regular Paper

On the Single-Atom Conductance of Ti

Nadia Parveen, Shu Kurokawa, and Akira Sakai*
Department of Materials Science and Engineering,
Kyoto University, Sakyo-ku, Kyoto 606-8501, Japan
(Received 4 July 2015; Accepted 16 September 2015; Published 3 October 2015)

Using non-equilibrium Green's function method, we have theoretically investigated electron transmission through [0001]-, [11$\bar{2}$0]-, and [1$\bar{1}$00]-oriented single-atom contacts (SACs) of Ti and found that all these SACs show transmission 2.3-2.4 at the Fermi level. The transmission sensitively varies with small perturbations of contact geometry but maintains its likeliest value at ~ 2. Our results are compared with the experimental conductance histogram of Ti observed in our previous work (e-J. Surf. Sci. Nanotech. **12**, 1 (2014)). [DOI: 10.1380/ejssnt.2015.435]

Keywords: Single-atom contacts; Conductance; HCP metals; Ti

I. INTRODUCTION

Single-atom contacts (SACs) of metals are the smallest of metal-metal contacts and considered as a potential candidate of interconnects in molecular and atomic scale devices. Because SACs are smaller than the mean free path of electrons, they manifest ballistic electron transport and show a conductance G that can be described by the Landauer formula [1],

$$G = G_0 \sum_i \tau_i = G_0 \tau\,, \qquad \tau = \sum_i \tau_i \qquad (1)$$

where $G_0 \equiv 2e^2/h$ is the quantum unit of conductance, and τ_i and τ are the transmission probability of the i-th conductance eigenchannel of an SAC and the total transmission, respectively. According to the work of Cuevas and coworkers [2], the number of conductance eigenchannels and their transmissions of an SAC are closely related to the valence state of the contact atom. SACs of monovalent metals such as Au, for example, has a single channel with $\tau \sim 1$. The Landauer formula then predicts $G \sim 1G_0$ for Au SACs as confirmed by many experiments in the past [1].

Although there have been numerous studies of metal SACs, most of them are on archetypal FCC metals such as Au and little has been known on SACs of non-FCC metals, except for 3d magnetic transition metals [3–5] and some refractory metals [6, 7]. Also unexplored is the SAC of HCP metals. Among HCP metals, the SAC conductance has been experimentally obtained on Mg [8], Zn [9] and Co [3, 4, 10, 11]. These experiments were conducted at 4 K or below, while most experiments made at 300 K somehow failed to produce SACs of Mg [8, 12], Zn [13] and Co [5]. In our recent experiment [14], we carried out break-junction experiments on Cd and Ti and obtained the conductance histogram shown in Fig. 1 for Ti contacts at 4 K. The histogram shows two peaks, the first peak at $0.9G_0$ and the second one at $2.1G_0$. The lowest conductance peak in a histogram usually corresponds to the smallest contact and customarily interpreted as the peak corresponding to an SAC. We therefore assigned the $0.9G_0$ peak as the SAC peak and concluded that the SAC conductance of Ti should be $0.9G_0$. A problem of our peak interpretation, as noted in our previous work [14], is that the assigned SAC conductance of Ti appears exceptionally low compared to that of other d-band transition metals which lies around $2G_0$ [3, 4]. For example, the SAC conductance of V, which is next to Ti in the periodic table, is $1.8G_0$ [15]. This urges us to reconsider about our previous peak assignment and evaluate the SAC conductance of Ti by carrying out theoretical calculations. In this work, we have calculated the electron transmission τ for Ti SACs and obtained the theoretical SAC conductance through Eq. (1). The results are compared with the observed conductance peaks in Fig. 1.

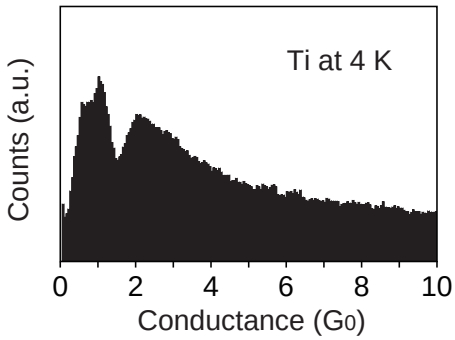

FIG. 1. Conductance histograms of Ti obtained at 4 K (adapted from Ref. [14]).

II. METHOD

Conductance calculations were made on three Ti SACs of different crystal orientations. Figure 2(a) shows the atomic arrangements of an SAC with its contact axis oriented along the [0001] direction. Both right and left electrodes have a pyramidal apex consisting of 11 atoms and the top atom of each apex makes a bond to form an SAC. In the [11$\bar{2}$0]- and [1$\bar{1}$00]-oriented SACs, apices are more flattened as shown in Figs. 2(b) and (c), respectively. In these SACs, the bonding distance between contact atoms are set equal to the nearest neighbor distance of Ti.

We employed ATK (Atomistix Toolkit) for evaluating the electron transmission through Ti SACs. Calculations are based on the NEGF (non-equilibrium Green's function) method in combination with DFT (density functional theory) techniques with GGA (generalized gradient approximation) for the exchange correlation. Recursion method [17] was used for the self-energy calculation. The

* Corresponding author: sakai.akira.4z@kyoto-u.ac.jp

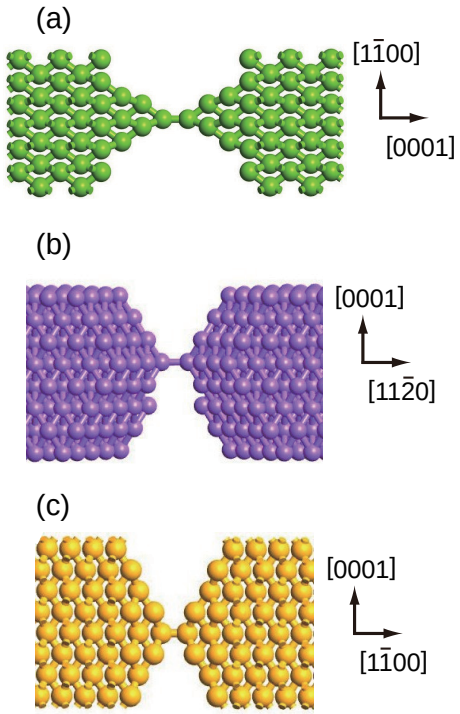

FIG. 2. Atomic structure of Ti SACs used for our transmission calculations. Panels (a), (b), and (c) represent the [0001]-, [11$\bar{2}$0]-, and [1$\bar{1}$00]-oriented Ti SACs, respectively.

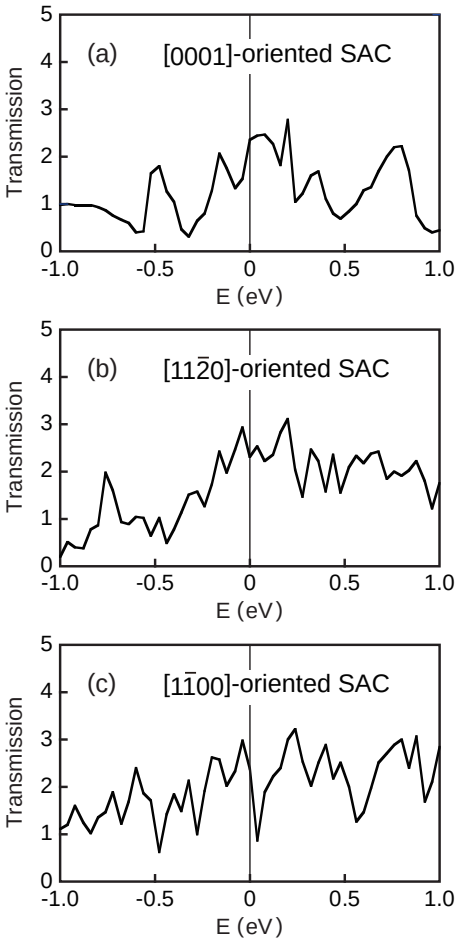

FIG. 3. Transmission spectrum obtained for each SAC shown in Fig. 2. Spectra (a)-(c) correspond to SACs (a)-(c) in Fig. 2, respectively. In each panel, the vertical line at $E = 0$ indicates the position of the Fermi level.

cut-off is 75 Hartree. We also assumed 300 K for electron temperature. The transmission spectrum was calculated for energies ± 2 eV from the Fermi level with a 3×3 k-point sampling. The recursion calculator was used for improving the accuracy of the results.

III. RESULTS AND DISCUSSION

We show in Fig. 3(a) the transmission spectrum calculated for the [0001]-oriented SAC of Fig. 2(a). The electron energy is measured from the Fermi level and the line at $E = 0$ in the plot indicates the position of the Fermi level. Previous calculations on some HCP SACs such as those of Mg [8] and Zn [16] yield relatively flat transmission spectra near the Fermi level, and the result is considered due to the *sp*-character of the valence electrons of these metals. On the other hand, the spectrum depicted in Fig. 3(a) shows many peak features, a characteristic presumably arising from the *d*-valency of Ti. At the Fermi level, the transmission is $\tau = 2.4$. Similar result is obtained for the [11$\bar{2}$0]- and [1$\bar{1}$00]-oriented SACs as shown in Figs. 3(b) and (c). The transmission spectrum exhibits many ups-and downs but again takes $\tau = 2.3 - 2.4$ at the Fermi level. This agreement of τ for three SACs of different orientations suggests that the transmission at the Fermi level little changes with the crystallographic orientation of SAC.

The SACs depicted in Fig. 2 are a dimer-SAC in a sense that right and left electrodes are connected by two single atoms. In addition to these dimer SACs, we also carried out transmission calculations on a monomer-SAC where right and left electrodes share a single Ti atom at their apices. Atomic geometry and the transmission spectrum of a [0001]-oriented monomer-SAC are shown in Fig. 4(a) and (b), respectively. As seen in the transmission spectrum, the monomer-SAC exhibits $\tau = 2.2$ at the Fermi level. This value is in good agreement with that of the dimer-SACs and suggests that the Fermi-level transmission appears little sensitive to the number of contact atoms.

On the other hand, we found appreciable variation of the transmission when positions of electrode atoms are slightly perturbed. To examine this influence of structural perturbation on the contact transmission, we randomly displaced 22 atoms in the right and left pyramidal electrodes of the [0001]-oriented SAC and calculated the transmission at the Fermi level. All displacements are kept less than 12.5 pm. Calculations were made for 30 such perturbed contact geometries and the resulting distribution of the transmission is shown in Fig. 5. As seen in the plot, small displacements of electrode atoms significantly change the transmission value from 1.1 to 2.5. Similar calculations made on *sp*-metals such as Mg [8] and Zn [16] SACs find no such sensitivity of the transmission to structural perturbations. We therefore consider that the observed variation of τ should be a characteristic of *d*-band SACs. In spite of the large variation of the transmission, however, the distribution shown in Fig. 5 still exhibits a clear peak at $\tau \sim 2.1$. Perturbations of atomic

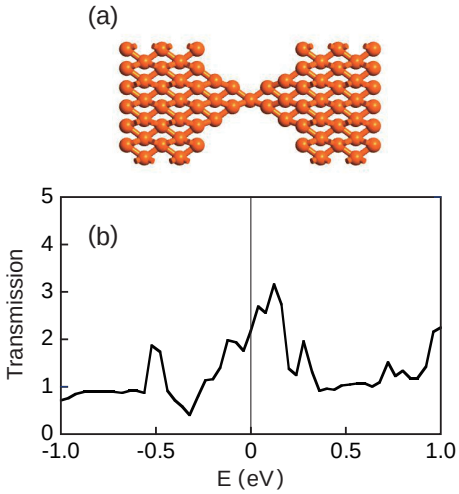

FIG. 4. Atomic geometry (a) and the transmission spectrum (b) of a [0001]-oriented monomer-SAC. As in Fig. 3, $E = 0$ corresponds to the Fermi level.

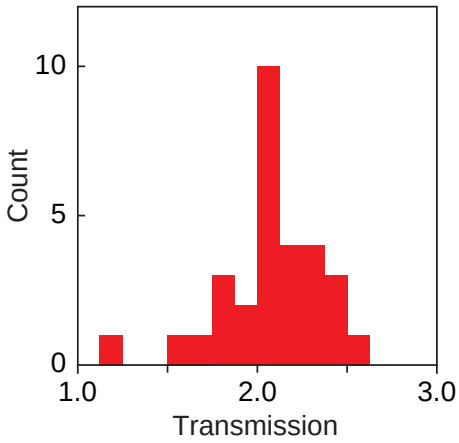

FIG. 5. Distribution of the transmission at the Fermi level obtained for 30 disturbed [0001]-oriented SACs. Atoms in the pyramidal part of each SAC are randomly displaced with the maximum displacement less than 12.5 pm.

positions can, therefore, broaden the transmission distribution but makes neither a large shift nor a smearing of the transmission peak.

The transmission discussed so far is the total transmission τ which is the sum of the transmission τ_i of each conductance eigenchannel as expressed in Eq. (1). Because the valence state of Ti is $3d^2 4s^2$, a Ti SAC should have four conductance eigenchannels. We carried out eigenchannel analyses at Γ-point for the [0001]-oriented SAC of Fig. 2(a) and in fact found four dominating channels. Their Fermi-level transmission is $\tau_1 = 0.97$, $\tau_2 = 0.91$, $\tau_3 = 0.15$, and $\tau_4 = 0.12$, respectively. Contributions from other channels are negligible. In SACs of trivalent Al, three *sp*-hybridized eigenchannels separate into one high-transmission and two low-transmission channels [18]. In Ti SACs, on the other hand, *sd*-hybridized eigenchannels yield two high- and two low-transmission channels, probably reflecting the difference between *p* and *d* valence electrons. Our τ values can also be compared with τ values of Nb SACs measured by Ludoph *et al.* [6], $\tau_1 = 0.81$, $\tau_2 = 0.67$, $\tau_3 = 0.63$, $\tau_4 = 0.33$, and $\tau_5 = 0.13$. Different from their results, our calculated τ shows high and low values but no intermediate transmissions. Such a disparity between theoretical and experimental transmissions is not, however, unexpected because atomic arrangements in real contacts should be less perfect than the idealized arrangements in theoretical models. In real contacts, high- and low-transmission channels might not be in full separation and channels of intermediate transmission would likely be developed. In the case of Al SACs, for example, theories [18] predict one high- and two low-transmission channels, while experiments [19] observed a couple of intermediate transmission channels.

We now compare our results with experiment. As shown in Fig. 1, the observed conductance histogram of Ti exhibit two peaks at $0.9G_0$ and $\sim 2G_0$, respectively. In our previous study, we assumed that the first peak at $0.9G_0$ would be the SAC peak of Ti. However, our results shown in Fig. 5 indicate that the transmission of Ti SACs is around 2 and unlikely to decrease to 0.9 even allowing small distortions in contact geometry. We can, therefore, conclude that the second peak, not the first one as assumed previously, would be the SAC conductance peak of Ti. The width of the second peak nearly corresponds to the broad distribution of the transmission shown in Fig. 5 and this also supports our new SAC peak assignment. As mentioned in Sec. I, most *d*-band transition metals show a broad SAC peak around $2G_0$. Our new SAC conductance of Ti is thus in line with those of other transition metals and resolves the aforementioned problem that the previously assumed $0.9G_0$ appears too low for the SAC conductance of Ti.

The peak assignment mentioned above, however, rises an alternate problem concerning the origin of the $0.9G_0$ peak in Fig. 1. Because Ti is a reactive metal and a well-known getter of various gases, a reasonable interpretation would be that the $0.9G_0$ peak comes from gas-affected SACs. In our previous study [14], we ruled out this possibility because the histogram shown in Fig. 1 was obtained at 4 K where no gases other than helium are present. It, however, remains a possibility that contaminant atoms might come from within the electrodes, not from environment. Among possible gas species that would give rise to the $0.9G_0$ peak, the likeliest candidate should be hydrogen because hydrogen is known for reducing the SAC conductance of various *d*-band transition metals from $\sim 2G_0$ to a value around $\sim 1G_0$ [11, 20–25]. Smit *et al.* [20] showed for hydrogenated Pt SACs that a hydrogen molecule is sandwiched by Pt electrodes to form a straight Pt–H–H–Pt contact. Following this adsorption geometry, we inserted a hydrogen molecule between two contact atoms of the [0001]-oriented SAC shown in Fig. 2(a) but found that the straight Ti–H–H–Ti contact is unstable. Hydrogen molecule appears dissociated and two H atoms move to the side of the electrode pyramids. Similar side attachment of hydrogen has been reported by Kiguchi *et al.* [25] for hydrogenated monomer Pd SACs. We, therefore, employed a monomer Ti SAC, placed two H atoms on the contact side, and carried out the energy optimization [26].

We show in Figs. 6(a) and (b) the resulting contact geometry and its transmission spectrum, respectively. The hydrogen atoms locates at the bridging site between the contact atom and the second-layer atom and nearly equidistant from them (0.185 nm and 0.175 nm, respectively). The H–H separation is 0.12 nm. The transmis-

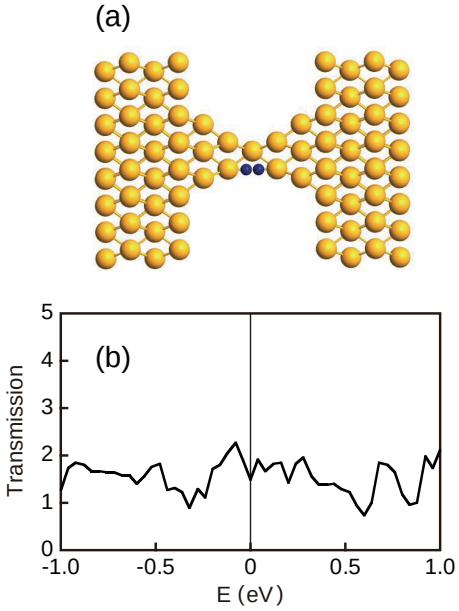

FIG. 6. Atomic structure (a) and the transmission spectrum (b) of the hydrogenated monomer SAC of Ti. Two small balls appearing in (a) represent hydrogen atoms. Compared with the clean monomer contact shown in Fig. 4(a), the contact is rotated around the contact axis to visualize the location of hydrogen atoms.

sion spectrum shown in Fig. 6(b) shows some fluctuations but appears less structured compared with the spectrum of the pure monomer SAC depicted in Fig. 4(b). No hydrogen-induced features can be recognized around the Fermi level. These results suggest that the attached hydrogen atoms do not form a new conduction pathway but strongly couples to Ti contact atoms. The transmission at the Fermi level decreases from $\tau = 2.2$ for the clean contact to $\tau = 1.5$. This transmission comes close to the lower edge of the transmission distribution of pure Ti shown in Fig. 5 and appears too high to account for the $0.9G_0$ peak. Eigenchannel transmissions at the Fermi level are also reduced as $\tau_1 = 0.53$, $\tau_2 = 0.47$, $\tau_3 = 0.30$, and $\tau_4 = 0.08$, respectively, so that the hydrogen adsorption nearly halves the transmissions of the two highly conducting eigenchannels of pure Ti SACs. On the other hand, the reduction of the total transmission remains 32% and falls short to explain the $0.9G_0$ peak. It should be noted, however, that these transmission values are obtained on one specific contact geometry based on the monomer Ti SAC of Fig. 4. Optimization of the adsorption configuration starting from different SACs would lead to different hydrogenated SACs and different transmissions. Considering the wide transmission distribution shown in Fig. 5, a few of those hydrogenated SACs would likely show lower transmissions close to 0.9. We cannot, therefore, exclude the possibility that the $0.9G_0$ peak is a hydrogen-induced peak. For unambiguously nailing down the origin of the $0.9G_0$ peak, further systematic studies should be made for various adsorption configurations and for gas species including hydrogen and oxygen [27] as well.

IV. SUMMARY

In our previous experiment [14], we observed two peaks in the conductance histogram of Ti contacts and, following the customary interpretation of the conductance peaks, assumed that the first peak at $0.9G_0$ would correspond to Ti SACs. Our transmission calculations on Ti SACs, on the other hand, show that the transmission at the Fermi level is $\tau = 2.3 - 2.4$. We tested the robustness of the transmission by putting small and random displacements on electrode atoms and found the broadening of the transmission as expected for d-band transition metals. However, the distribution of the transmission still exhibits a sharp peak at $\tau \sim 2$. These results suggest that the second peak at $2.1G_0$ in the histogram, not the first one as assumed before, would be the SAC peak of Ti and the SAC conductance of Ti should thus be $\sim 2G_0$. Our new value is in accord with those of other d-band transition metals and resolves the problem that $0.9G_0$ is seemingly too low for the SAC conductance of Ti.

ACKNOWLEDGMENTS

We are deeply indebted to Mr. Shinji Usui of QuantumWise Japan for his full range of technical assistance for our transmission calculations.

[1] N. Agraït, A. Levy Yeyati, and J. M. van Ruitenbeek, Phys. Rep. **377**, 81 (2003).
[2] J. C. Cuevas, A. Levy Yeyati, and A. Martín-Rodero, Phys. Rev. Lett. **80**, 1066 (1998).
[3] C. Untiedt, D. M. T. Dekker, D. Djukic, and J. M. van Ruitenbeek, Phys. Rev. B **69**, 081401(R) (2004).
[4] M. R. Calvo, J. Fernández-Rossier, J. J. Palacios, D. Jacob, D. Natelson, and C. Untiedt, Nature (London) **458**, 1150 (2009).
[5] Y. Moriguchi, K. Yamauchi, S. Kurokawa, and A. Sakai, Surf. Sci. **606**, 928 (2012).
[6] B. Ludoph, N. van der Post, E. N. Bratus, E. V. Bezuglyi, V. S. Shumeiko, G. Wendin, and J. M. van Ruitenbeek, Phys. Rev. B **61**, 8561 (2000).
[7] D. den Boer, O. I. Shklyarevskii, and S. Speller, Physica B **395**, 20 (2007).
[8] R. H. M. Smit, A. I. Mares, M. Häfner, P. Pou, J. C. Cuevas, and J. M. van Ruitenbeek, New J. Phys. **11**, 073043 (2009).
[9] E. Scheer, P. Konrad, C. Bacca, A. Mayer-Gindner, H. V. Löhneysen, M. Häfner, and J. C. Cuevas, Phys. Rev. B **74** 205430 (2006).
[10] H. Egle, C. Bacca, H.-F. Pernau, M. Huefner, D. Hinzke, U. Nowak, and E. Scheer, Phys. Rev. B **81**, 134402 (2010).
[11] T. Nakazumi and M. Kiguchi, J. Phys. Chem. Lett. **1**, 923 (2010).
[12] A. Takahashi, S. Kurokawa, and A. Sakai, Phys. Status Solidi A **209**, 2151 (2012).

[13] R. Suzuki, Y. Mukai, M. Tsutsui, S. Kurokawa, and A. Sakai, Jpn. J. Appl. Phys. **45**, 7217 (2006).
[14] T. Horiuchi, A. Takahashi, S. Kurokawa, and A. Sakai, e-J. Surf. Sci. Nanotech. **12**, 1 (2014).
[15] A. I. Yanson, Ph.D. thesis, University of Leiden (2000).
[16] M. Häfner, P. Konrad, F. Pauly, J. C. Cuevas, and E. Scheer, Phys. Rev. B **70**, 241404R (2004).
[17] M. P. Lopez Sancho, J. M. Lopez Sancho, and J. Rubio, J. Phys. F, **15**, 851 (1985).
[18] N. Kobayashi, M. Brandbyge, and M. Tsukada, Phys. Rev. **B 62**, 8430 (2000).
[19] E. Scheer, P. Joyez, D. Esteve, C. Urbina, and M. H. Devoret, Phys. Rev. Lett. **78**, 18 (1997).
[20] R. H. M. Smit, Y. Noat, C. Untiedt, N. D. Lang, M. C. van Hemert and J. M. van Ruitenbeek, Nature **419**, 906 (2002).
[21] Sz. Csonka, A. Halbritter, G. Mihály, O. I. Shklyarevskii, S. Speller and H. van Kempen, Phys. Rev. Lett. **93** 016802 (2004).
[22] M. Kiguchi, R. Stadler, I. S. Kristensen, D. Djukic, and J. M. van Ruitenbeek, Phys. Rev. Lett. **98** 146802 (2007).
[23] D. den Boer, O. I. Shklyarevskii, J. A. A. W. Elemans, and S. Speller, Phys. Rev. B **77**, 165423 (2008).
[24] P. Makk, Sz. Csonka, and A. Halbritter, Phys. Rev. B **78**, 045414 (2008).
[25] M. Kiguchi, K. Hashimoto, Y. Ono, T. Taketsugu, and K. Murakoshi, Phys. Rev. B **81**, 195401 (2010).
[26] The energy optimization has been made for a smaller contact that consists of two pyramids and two hydrogen atoms.
[27] W. H. A. Thijssen, M. Strange, J. M. J. aan de Brugh, and J. M. van Ruitenbeek, New J. Phys. **10**, 033005 (2008).